



Adaptive stability transformation method of chaos control for first order reliability method

Zeng Meng¹ · Yuxue Pu¹ · Huanli Zhou¹

Received: 19 July 2017 / Accepted: 17 November 2017 / Published online: 24 November 2017
© Springer-Verlag London Ltd., part of Springer Nature 2017

Abstract

The efficiency and robustness are two key performance indexes for first-order reliability method (FORM). In this study, two different algorithms, including the adaptive stability transformation method (ASTM) and enhanced adaptive stability transformation method (EASTM), are proposed to improve the efficiency and robustness of FORM. In both ASTM and EASTM, the computation of most probable failure point (MPFP) is converted to find a series of most probable target points (MPTPs), in which the chaos control factor is properly selected by proposing two different algorithms. Four benchmark examples with normal and non-normal random variables and one practical engineering application example are tested to verify the effectiveness of the proposed algorithms. The results illustrate that the proposed algorithms not only are more efficient than other advanced FORM algorithms, but also are very robust.

Keywords First-order reliability method · Stability transformation method · Most probable failure point · Most probable target point

1 Introduction

Uncertainty propagation extensively exists in structural and mechanical engineering system, which should be addressed to guarantee the structural safety with uncertainty factors [1–3]. To satisfy the reliability requirement at the product design phase, its reliability should be computed to handle these uncertainties by formulating the performance function with random variables [4, 5]. There are many existing methods to evaluate the structure reliability, in which the most probable failure point (MPFP) based methods are one popular type [6]. This type of method evaluates the failure of probability at MPFP by solving the formulation of first-order reliability method (FORM). Actually, FORM is one of the most commonly utilized method in the domains of reliability assessment and reliability-based design optimization (RBDO) because of the high performance of the applicability, efficiency and robustness [7–10]. Besides, performance measure approach (PMA) is also extensively used in RBDO

by computing the most probable target point (MPTP) due to its efficiency and robustness [11, 12].

Until now, a series of MPFP algorithms have been put forward to search MPFP. Hasofer and Lind [13] and Rackwitz and Fiessler [14] introduced the HL–RF algorithm to compute the MPFP. However, it often meets the non-convergence problem and shows the bifurcation, periodic oscillation and chaotic phenomena for nonlinear problem. To address the issue, a series of improved algorithms were developed consecutively, such as *i*HL–RF, *n*HL–RF, full characterization method. [15–17]. Among them, *i*HL–RF and *n*HL–RF are the two robust methods by given a proper iterative step, but they are inefficient for solving nonlinear problems [15, 18]. Yang et al. [19] indicated that the non-convergence problem of HL–RF algorithm not only is impacted by the curvature value and nonlinearity of limit state function, but also is related to the system property. Then, the stability transformation method (STM) based on chaos theory is used to search the MPFP stably. However, it also shows low convergence rate.

More recently, Meng et al. [20] found that the iteration point of HL–RF algorithm has the directional property, and then the efficiency of STM is improved significantly by proposing directional stability transformation method (DSTM). Moreover, other advanced iterative algorithms,

✉ Zeng Meng
mengz@hfut.edu.cn

¹ School of Civil Engineering, Hefei University of Technology, Hefei 230009, People's Republic of China

such as conjugate finite-step length method [21], chaotic conjugate stability transformation method [22] and limited Fletcher–Reeves (LFR) method [23], are developed to improve the robustness of MPFP search. All these improved algorithms calculate the MPFP directly by solving a complex nonlinear constraint [24]. On the other hand, it is commonly acknowledged that PMA is more efficient and robust than MPFP search method by solving a simple constraint [11, 12]. Thus, if the concept of PMA can be applied to compute the MPFP, the performance of these algorithms can be enhanced.

This paper is dedicated to improve the efficiency and robustness of MPFP search algorithm through proposing two novel algorithms: adaptive stability transformation method (ASTM) and enhanced adaptive stability transformation method (EASTM). The basic idea of the proposed algorithms is that the MPFP search model is converted into MPTP search model. Based on the DSTM, the reliability analysis model is further simplified to the unconstraint optimization model, and then the MPFP is searched efficiently and robustly. Furthermore, EASTM is developed by estimating the approximate MPTP, so the efficiency is further improved without sacrificing its robustness.

2 The concept of FORM

FORM evaluates the probability of failure by solving an optimization model [18] that is formulated as

$$\begin{aligned} \min_U \quad & \|U\| \\ \text{s.t.} \quad & G(U) = 0, \end{aligned} \tag{1}$$

where $U \in R^n$ is the vector of random variables in standard normal space (U-space). The optimum U^* is named as most probable failure point (MPFP) that is the closest point from origin to the limit state surface, as shown in Fig. 1a. Then, the reliability is measured by the distance between design

point and origin. The probability of failure can be calculated by the formulation: $P_f = \Phi(-\beta) = \Phi(-\|U^*\|)$.

Tu and Choi [25] introduced the PMA of FORM to solve RBDO problem, the formulation is as follows:

$$\begin{aligned} \min_U \quad & G(U) \\ \text{s.t.} \quad & \|U\| = \beta^t, \end{aligned} \tag{2}$$

where β^t is the target reliability index. The optimum in Eq. (2) is called as the most probable target point (MPTP). It represents the minimum value of performance function at the target reliability surface, as shown in Fig. 1b. It has been proved that the calculation of PMA is more efficient and robust than that of reliability index approach [11, 12]. Therefore, we attempt to enhance the efficiency and robustness of MPFP search algorithm by transforming it to finding MPTP. This is introduced in Sect. 5.

3 The iterative algorithms of FORM

3.1 HL–RF algorithm

The MPFP search methods solve the FORM problem, and then the structural probability of failure is obtained. The reliability of FORM is evaluated by the reliability index β , and MPFP is the closest point from origin to the limit state surface [1]. The probability of failure can be evaluated by reliability index as follows:

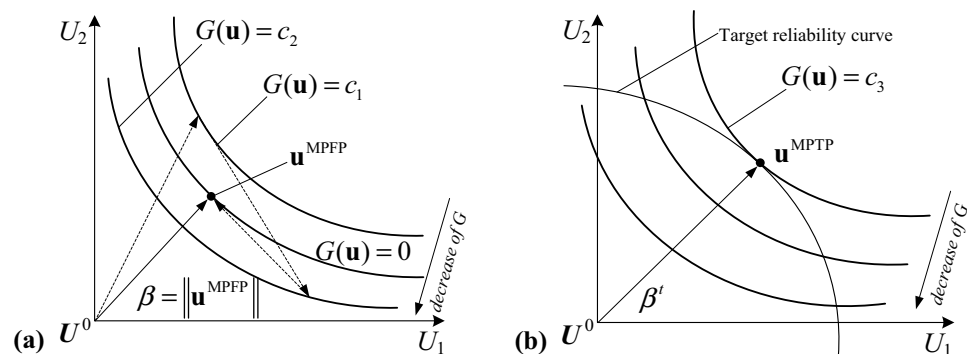
$$P_f = \Phi(-\beta) = \Phi(-\|U^*\|), \tag{3}$$

where Φ is the cumulative distribution function in standard normal space (U-space). Assume the performance function is

$$Z = g(X) = g(X_1, X_2, \dots, X_n). \tag{4}$$

The HL–RF algorithm of FORM is expressed as follows:

Fig. 1 a MPFP search process. b MPTP search process



$$U^{k+1} = \frac{(\nabla g(U^k))^T U^k - g(U^k)}{(\nabla g(U^k))^T \nabla g(U^k)} \nabla g(U^k), \tag{5}$$

where $U \in R^n$ is the vector of random variables in U-space. The mean and standard deviation are μ and σ , respectively. If the random variable vector X follows the normal distribution, then it can be calculated by $X = \mu + \sigma U$. Otherwise, when random variable vector follows the non-normal distribution, the random variables should be transformed to standard normal variables. As shown in Fig. 2a, if HL–RF is used for solving nonlinear problems, the iterative point appears oscillation or non-convergence phenomenon. Thus, other improved algorithms, including *i*HL–RF and CC methods, are developed to overcome this problem.

3.2 *i*HL–RF iterative algorithm

*i*HL–RF iterative algorithm is widely used for evaluating the reliability due to its efficiency and stability [6]. The iterative formulation is constructed based on the merit function.

$$U^{k+1} = U^k + \alpha d^k, \tag{6}$$

where d^k is the search direction and is computed by

$$d^k = \frac{(\nabla g(U^k))^T U^k - g(U^k)}{(\nabla g(U^k))^T \nabla g(U^k)} \nabla g(U^k) - U^k. \tag{7}$$

The iterative step length is decided by solving the following merit function:

$$\begin{cases} m(U) = \frac{1}{2} \|U\| + c|G(U)| \\ c > \frac{\|U\|}{\|\nabla G(U)\|} \end{cases}, \tag{8}$$

where c is the constant. Here, c is selected as $c = \frac{\|U\|}{\|\nabla G(U)\|} + 10$, according to the reference [6].

4 Iterative algorithms based on the chaos control theory

4.1 Stability transformation method

Chaos control theory has been adopted successfully to eliminate the unstable phenomena of iterative algorithms [26, 27]. Yang [24] introduced the stability transformation method (STM), which stabilizes the unstable fixed points of dynamical system by modifying the eigenvalues of Jacobian matrix [28]. The formulation is described as

$$U^{k+1} = U^k + \lambda^k C(f(U^k) - U^k), \tag{9}$$

$$f(U^k) = \frac{(\nabla g(U^k))^T U^k - g(U^k)}{(\nabla g(U^k))^T \nabla g(U^k)} \nabla g(U^k), \tag{10}$$

where f is the vector of iterative function. U^k is the m -dimensional random variables at the k th iterative step. C is the $m \times m$ -dimensional involutory matrix, and the elements in each row and each column have only one element with value of 1 or -1 and the other elements are 0. So the total number of involutory matrix is $2^m m!$. The control factor λ^k is the range $[0, 1]$ and is determined by the spectral radius of the original system’s Jacobian matrix. The larger the spectral radius of Jacobian matrix is, the smaller the control factor λ should be selected to achieve stability. Specially, when $C = I$, Eq. (9) becomes

$$U^{k+1} = U^k + \lambda^k (f(U^k) - U^k). \tag{11}$$

A two-dimensional example is shown in Fig. 2b. It is found that STM achieves the stability by reducing the iterative step size. Since every step size is controlled strictly, it is inefficient for MPFP search. To address this issue, the DSTM is developed by adopting the directional chaos control strategy, which will be introduced in the next section.

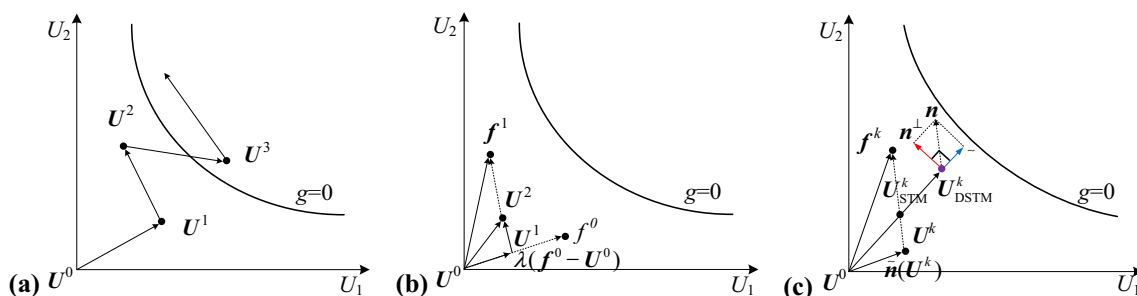


Fig. 2 a HL–RF iterative process. b STM iterative process. c DSTM iterative process

4.2 Directional stability transformation method

Recently, Meng et al. [20] pointed out that the oscillation of iterative point has directional property, and then the DSTM is suggested to improve the efficiency. As shown in Fig. 2c, the oscillation is mainly incurred by circumferential direction $n^\perp(U^k)$ other than radial direction $\tilde{n}(U^k)$. The formulation of DSTM is depicted as

$$\begin{aligned}
 U^{k+1} &= \beta^k \frac{\tilde{n}(U^{k+1})}{\|\tilde{n}(U^{k+1})\|} \\
 \beta^k &= \frac{(\nabla g(U^k))^T U^k - g(U^k)}{(\nabla g(U^k))^T \nabla g(U^k)} \\
 \tilde{n}(U^k) &= U^k + \lambda^k C(f(U^k) - U^k),
 \end{aligned}
 \tag{12}$$

where $\tilde{n}(U^k)$ is the vector of radial direction. β^k is the reliability index at the k th iterative step. Since all parameters of DSTM can be obtained by original STM, it is very convenient for engineering application. However, a proper control factor λ^k should be provided to guarantee the robustness and efficiency of DSTM. If the control factor is too large, the results of DSTM may lead to non-convergence. Otherwise, if the control factor is too small, it requires too much computational cost. Therefore, the improved MPFP search methods should be suggested, which is introduced in Sect. 5.

5 Adaptive stability transformation method

Although DSTM improves the efficiency of STM significantly, it must select a proper chaos control factor. If the chaos control factor is too large, the iterative point may lead to non-convergence. On the contrary, if the chaos control factor is too small, it needs to much computational cost. Therefore, how to select a proper chaos control factor is crucial.

Property 1 For DSTM, the iterative point at the $k + 1$ th iterative step is located at hyper-sphere with radius equal to β^k .

Proof From Eq. (12), it is found that

$$\begin{aligned}
 U^{k+1} (U^{k+1})^T &= \beta^k \frac{\tilde{n}(U^{k+1})}{\|\tilde{n}(U^{k+1})\|} \beta^k \frac{\tilde{n}(U^{k+1})^T}{\|\tilde{n}(U^{k+1})\|} \\
 &= \beta^{k2} \frac{\tilde{n}(U^{k+1}) \tilde{n}(U^{k+1})^T}{\|\tilde{n}(U^{k+1})\|^2} \\
 &= \beta^{k2}.
 \end{aligned}$$

Then, the radius of hyper-sphere $\|U^{k+1}\| = \beta^k$. Thus, Property 1 has been proved.

From the definition of reliability analysis model and PMA, it is observed that the direction $U_{MPFP} - U_{MPTP}^{k+1}$ represents the steepest descent direction at the hyper-sphere with radius $\|U_{MPTP}^{k+1}\|$, as shown in Fig. 3. Especially, when β computed by Eq. (1) is equal to β' in Eq. (2), the MPFP and MPTP become the same point. Then, the reliability analysis model can be converted into the optimization model of PMA. From Property 1, the best chaos control factor at the k th iterative step that can be estimated by solving the following optimization formulation:

$$\begin{aligned}
 \min_{\lambda^k} & G(U^{k+1}(\lambda^k)) \\
 \text{s.t.} & \|U^{k+1}\| = \beta^k,
 \end{aligned}
 \tag{13}$$

where λ^k is deemed as the design variable in Eq. (13). According to property 1, the equality constraint $\|U\| = \beta^k$ is satisfied naturally. Then we substitute the Eq. (12) into Eq. (13), the optimization model of Eq. (13) can be further simplified as an unconstraint optimization model with only one design variable λ^k ,

$$\min_{\lambda^k} G \left(\beta^k \frac{U^k + \lambda^k C(f(U^k) - U^k)}{\|U^k + \lambda^k C(f(U^k) - U^k)\|} \right).
 \tag{14}$$

Here the Eq. (14) can be solved by classical gradient algorithm, such as sequential quadratic programming (SQP). To solve the optimization model conveniently, the sensitivity of

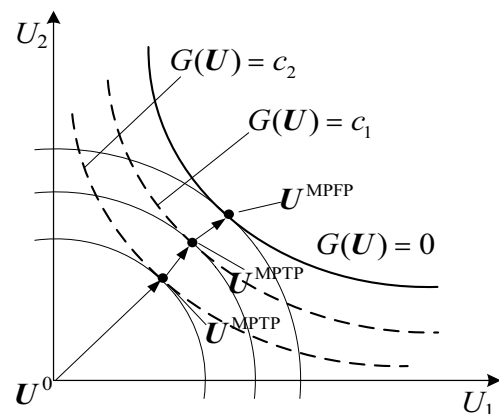


Fig. 3 ASTM iterative process

objective function should be offered. According to chain rule, the sensitivity is as follows:

$$\frac{dG}{d\lambda^k} = \beta^k \left(\frac{\lambda^k \mathbf{C}(\mathbf{f}(\mathbf{U}^k) - \mathbf{U}^k)}{\|\mathbf{U}^k + \lambda^k \mathbf{C}(\mathbf{f}(\mathbf{U}^k) - \mathbf{U}^k)\|} - \frac{\lambda [\mathbf{U}^k + \lambda^k \mathbf{C}(\mathbf{f}(\mathbf{U}^k) - \mathbf{U}^k)] [\mathbf{C}(\mathbf{f}(\mathbf{U}^k) - \mathbf{U}^k)]^T [\mathbf{U}^k + \lambda^k \mathbf{C}(\mathbf{f}(\mathbf{U}^k) - \mathbf{U}^k)]}{\|\mathbf{U}^k + \lambda^k \mathbf{C}(\mathbf{f}(\mathbf{U}^k) - \mathbf{U}^k)\|^3} \right)^T \tag{15}$$

When involutory matrix \mathbf{C} is set as the unit matrix \mathbf{I} , the Eq. (15) becomes

$$\frac{dG}{d\lambda^k} = \beta^k \left\{ \frac{\lambda^k (\mathbf{f}(\mathbf{U}^k) - \mathbf{U}^k)}{\|\tilde{\mathbf{n}}(\mathbf{U}^{k+1})\|} - \frac{\lambda^k \tilde{\mathbf{n}}(\mathbf{U}^{k+1}) (\mathbf{f}(\mathbf{U}^k) - \mathbf{U}^k)^T \tilde{\mathbf{n}}(\mathbf{U}^{k+1})}{\|\tilde{\mathbf{n}}(\mathbf{U}^{k+1})\|^3} \right\}^T \tag{16}$$

Since the vectors $\tilde{\mathbf{n}}(\mathbf{U}^{k+1})$, $\mathbf{f}(\mathbf{U}^k)$ and \mathbf{U}^k are already obtained from the previous iterative step, the sensitivity can be calculated simply without generating additional computational cost. Then, the SQP can be used to compute the chaos control factor, and the optimization model of Eq. (14) can be rewritten by Taylor expansion at the current chaos control factor λ^k ,

$$\min_{\lambda} \quad G + \frac{dG}{d\lambda^k} (\lambda - \lambda^k) + \frac{d^2\tilde{G}}{d\lambda^{k2}} \frac{(\lambda - \lambda^k)^2}{2}, \tag{17}$$

where $\frac{dG}{d\lambda^k}$ is the first order derivative, $\frac{d^2\tilde{G}}{d\lambda^{k2}}$ is the approximate second order sensitivity that can be computed by symmetric rank-one update [5]. Based on Eq. (17), the chaos control factor can be solved easily. Although ASTM can solve the nonlinear problem, it may show inefficiency for

linear problems. Thus, the following update criterion is constructed to overcome this problem for ASTM:

$$\zeta^{k+1} = (\mathbf{U}^{k+1} - \mathbf{U}^k)(\mathbf{U}^k - \mathbf{U}^{k-1})^T$$

$$\text{sgn}(\zeta^{k+1}) > 0 : \quad \text{Not oscillation} \tag{18}$$

$$\leq 0 \quad \text{Oscillation,}$$

where \mathbf{U}^k represents the iterative random point of ASTM at the k th step. $\text{sgn}(\cdot)$ is the sign function. As shown in Fig. 4, if $\cos \theta^{k+1}$ is less than zero, it means that the vectors $\mathbf{U}^{k+1} - \mathbf{U}^k$ and $\mathbf{U}^k - \mathbf{U}^{k-1}$ have the same descent direction and the iterative point does not oscillate during the iterative process. If $\cos \theta^{k+1}$ is larger or equal to zero, the vectors $\mathbf{U}^{k+1} - \mathbf{U}^k$ and $\mathbf{U}^k - \mathbf{U}^{k-1}$ are in the opposite descent direction and the iterative point is oscillatory during the iterative process. The formulations of Eqs. (12) and (13) are applied to search MPFP and a middle value 0.5 is selected as the initial value of chaos control factor to achieve a better efficiency. Otherwise, the HL–RF iterative algorithm is employed. In general, the flowchart of ASTM is shown in Fig. 5a and the procedures are as follows:

- Step 1: Initialize the random variables \mathbf{X}^0 .
- Step 2: Transform the random variables \mathbf{X}^k to standard normal variables \mathbf{U}^k .

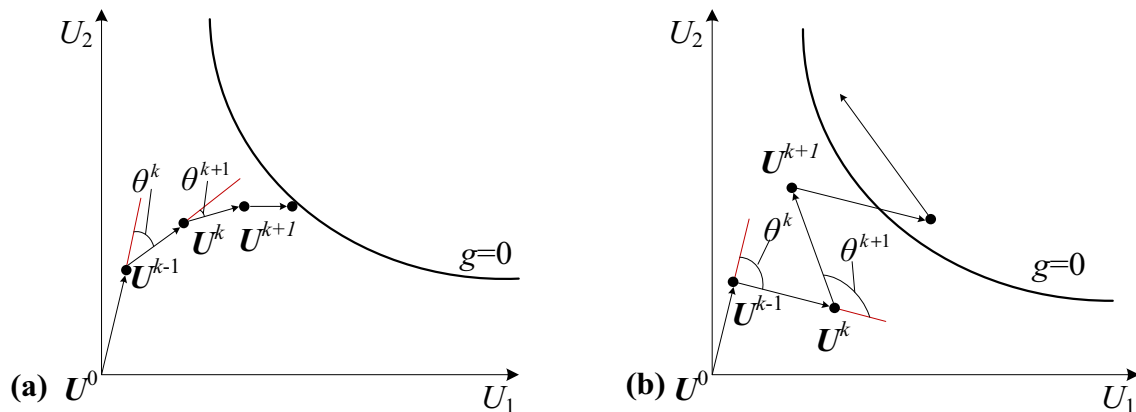


Fig. 4 Oscillation-checking criterion. a Not oscillation. b Oscillation

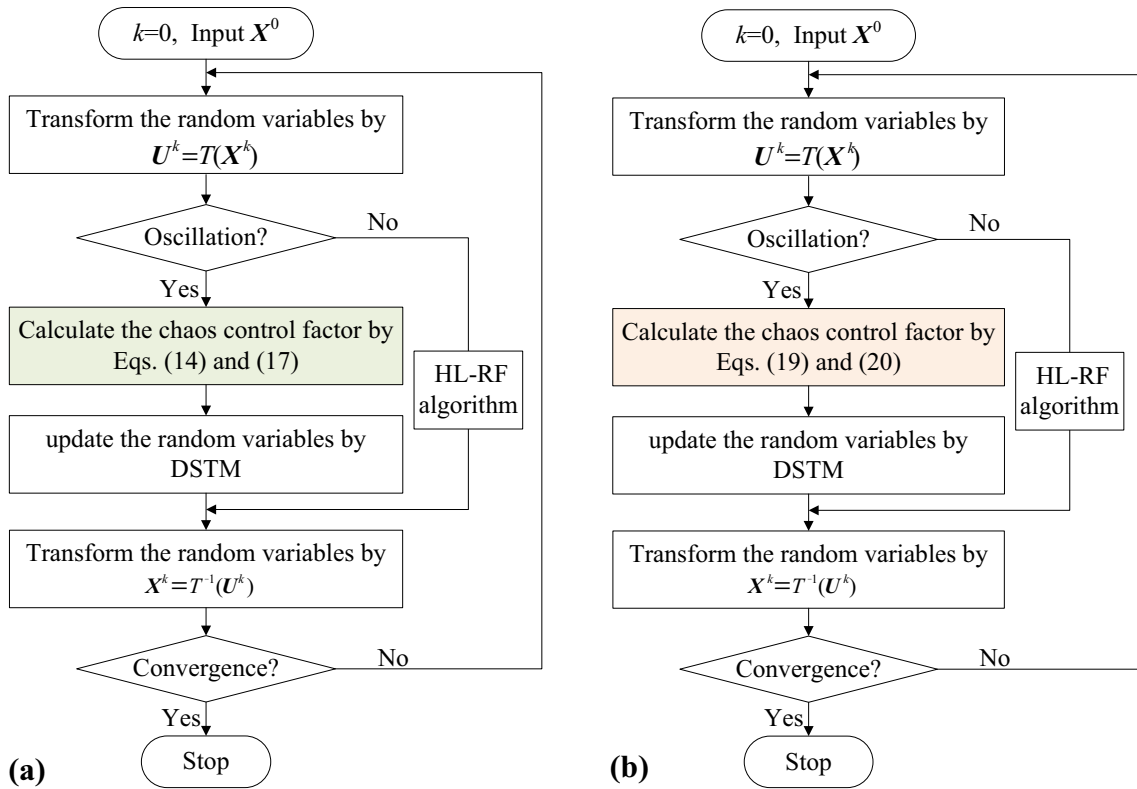


Fig. 5 a Flowchart of ASTM. b Flowchart of EASTM

- Step 3: Identify the oscillation of the random variables by Eq. (18).
- Step 4: If the iterative point does not oscillate during the iterative process, the random variables are updated using HL–RF algorithm of Eq. (5). Once the iterative point oscillates in the iterative process, the chaos control factor is updated by Eqs. (14) and (17). The random variables are calculated by DSTM using Eq. (12).
- Step 5: Transform the standard normal variables U^k to random variables X^k .
- Step 6: If convergent, stop; otherwise, go to step 2.

6 Enhanced adaptive stability transformation method

Although ASTM determines the chaos control factor adaptively, it requires solving a complete optimization model to obtain the chaos control in each iterative step. Thus, the enhanced adaptive stability transformation method (EASTM) is further developed to avoid the optimization process. Here we use the angle ratio between the current and previous angles to update the chaos control factor. As shown in Fig. 4, when the angles between two consecutive iterative points decrease gradually, i.e., $\theta^{k+1} \leq \theta^k$, the iterative point converges to the optimum without oscillation. Thus,

the chaos control factor does not required update. Otherwise, when the angel increases during the iterative process, i.e., $\theta^{k+1} > \theta^k$, the iterative process appears oscillation. Thus, the value of chaos control factor should be decreased to achieve stability. Then, the angle ratio θ^k / θ^{k+1} is used to reduce the value of chaos control factor. To avoid the update of the chaos control too strictly, the minimum value of angle ratio $\eta_\theta = \theta^k / \theta^{k+1}$ is set to be 0.4. Then, the formulation is described as follows:

$$\lambda = \begin{cases} \max[\lambda^{\theta^k / \theta^{k+1}} \eta_\theta \lambda] & \theta^{k+1} > \theta^k \\ \lambda & \theta^{k+1} \leq \theta^k \end{cases} \tag{19}$$

where angel θ^k is evaluated by

$$\theta^k = \arccos \left(\frac{U^k \cdot (U^k - U^{k-1})^T}{\|U^k\| \|U^k - U^{k-1}\|} \right) \tag{20}$$

In EASTM, the approximate MPFP is computed to avoid solving the optimization formulation of Eq. (14). Therefore, the computational cost of MPFP search can be further reduced. Because the EASTM is only utilized when the iterative point is oscillatory, a middle value 0.5 is selected as initial value of chaos control factor. In general, both ASTM

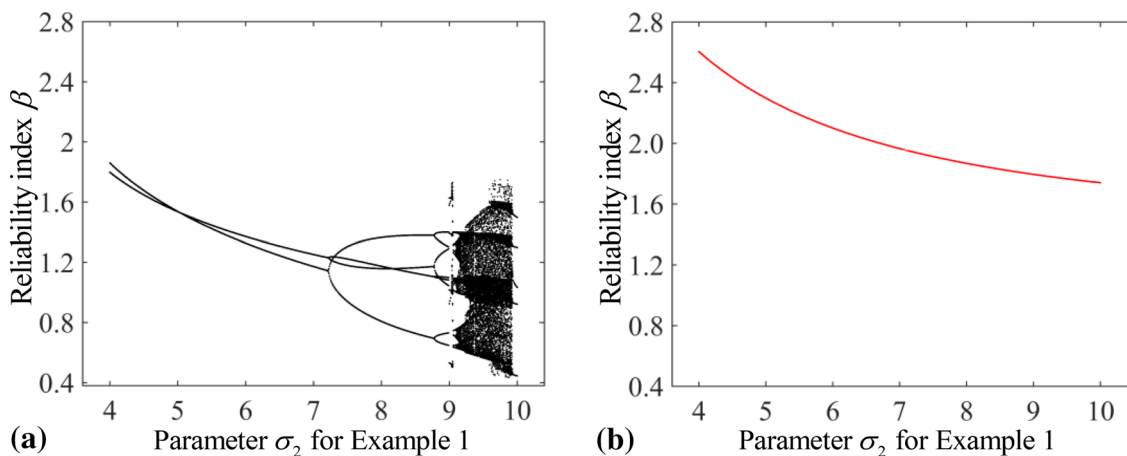


Fig. 6 **a** Bifurcation plot of reliability index of Example 1 using the HL–RF algorithm. **b** Chaos control of the HL–RF algorithm of Example 1 using STM and EASTM

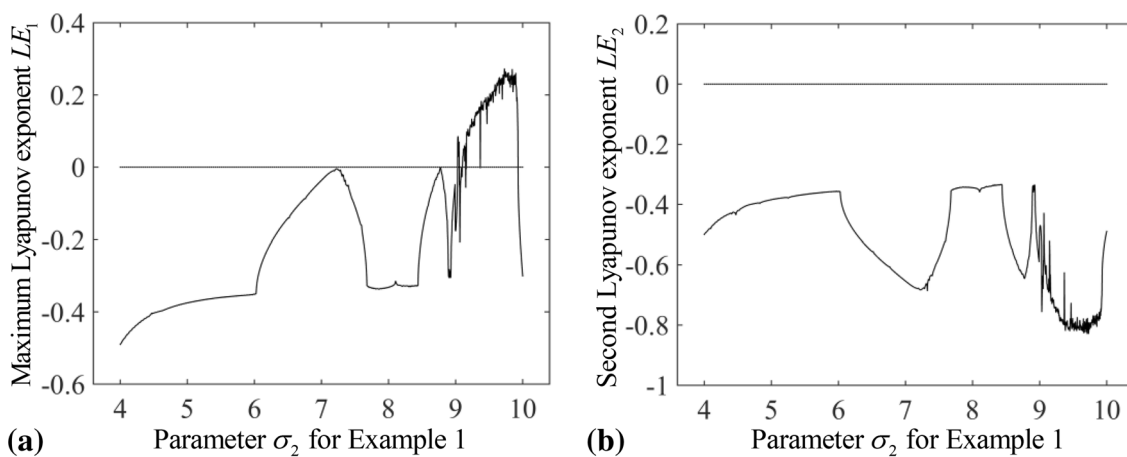


Fig. 7 Two Lyapunov exponents of the HL–RF algorithm for Example 1

and EASTM can compute the MPTP efficiently. The flow-chart is shown in Fig. 5b. The procedures of EASTM are identical to ASTM except that the chaos control factor is computed by Eqs. (19) and (20).

7 Illustrative examples

In this section, five examples with nonlinear performance function are carried on by the proposed ASTM and EASTM and are compared by other five popular iterative algorithms, including HL–RF, *i*HL–RF, LFR, STM and DSTM algorithms. The chaos control factors of both STM and DSTM are set to be 0.05. The initial point is the mean of the random variables, and the stopping criterion is 10^{-4} ($\|X^k - X^{k-1}\| / \|X^k\| \leq 10^{-4}$) for all these algorithms.

Table 1 The number of function evaluations of different algorithms for Example 1

Methods	MPFP	Iterations	F evaluations	β	β^{Mcs}
HL–RF	–	–	–	–	2.5234
<i>i</i> HL–RF	(1.6855, 1.9679)	31	280	2.2983	2.5234
STM	(1.6855, 1.9679)	202	606	2.2983	2.5234
DSTM	(1.6855, 1.9679)	25	75	2.2983	2.5234
LFR	(1.6855, 1.9679)	20	60	2.2983	2.5234
ASTM	(1.6855, 1.9679)	8	38	2.2983	2.5234
EASTM	(1.6855, 1.9679)	9	27	2.2983	2.5234

Example 1 $g_1 = X_1^3 + X_1^2 X_2 + X_2^3 - 18$, in which X_1 and X_2 represent the random variables with normal distribution, $\mu_1 = 10, \mu_2 = 9.9, \sigma_1 = \sigma_2 = 5$ [24].

The standard deviation σ_2 is deemed as the control parameter that is used to demonstrate the convergence of HL–RF algorithm. The bifurcation plot of reliability index of HL–RF algorithm and two Lyapunov exponents are given in Figs. 6 and 7, respectively, which are identical to reference [20]. If all Lyapunov exponents are less than 0, it means that the HL–RF algorithm has periodic or fixed solutions. Otherwise, if the maximum Lyapunov exponent is less than 0, the solution is unstable and generates chaotic solutions. From Figs. 6 and 7, it is seen that the reliability index β shows the bifurcation, chaos and periodic oscillation phenomena as the change of parameter σ_2 , and the Lyapunov exponents reflect these phenomena strictly.

The results of all different algorithms are listed in Table 1, and the F evaluations denotes the number of function calls. In addition, Monte Carlo simulation (MSC) is used to verify outcomes of different methods with a 10-million sample size. It is found that all these FORM methods have some errors for this highly nonlinear limit state function, and the second-order reliability method (SORM) can be further utilized to improve the accuracy. From Table 1,

all these methods except HL–RF iterative algorithm converge to the same optimum. *i*HL–RF and STM algorithms are robust but not efficient. The DSTM is more efficient than LFR, STM and *i*HL–RF using the directional chaos control strategy. Comparing with other algorithms, the efficiency of ASTM and EASTM is improved significantly by taking advantage of MPTP search. Although the number of iterations of ASTM is less than that of EASTM, ASTM needs calling performance function 28 times to obtain the chaos control factor. So EASTM is the more efficient than ASTM because it avoids entire optimization model for determining chaos control factor. In addition, the impact of different minimum angle ratios $\eta_{\theta\theta}$ and initial chaos control factor λ_0 for EASTM is investigated, and the results are listed in Table 2. When large values of $\eta_{\theta\theta}$ and λ_0 are related, the EASTM meets the convergence problem. On the contrary, when the values of two parameters are too small, the EASTM is inefficient. As evident from Table 2, the middle values $\lambda_0 = 0.5$ and $\eta_{\theta} = 0.4$ are very promising for EASTM.

Example 2 $g_2 = e^{1+\alpha X_1 - X_2} + e^{5-5\alpha X_1 - X_2} - 1$, in which $\alpha = 0.4$, both X_1 and X_2 represent the random variables with normal distribution, $\mu_1 = 0, \mu_2 = 0, \sigma_1 = \sigma_2 = 1$ [6].

The standard deviation σ_1 is deemed as the control parameter, which is used to demonstrate the convergence

Table 2 The impact of different minimum angle ratios η_{θ} and initial chaos control factor λ_0

λ_0	$\eta_{\theta} = 0.1$	$\eta_{\theta} = 0.2$	$\eta_{\theta} = 0.4$	$\eta_{\theta} = 0.5$	$\eta_{\theta} = 0.6$	$\eta_{\theta} = 0.8$	$\eta_{\theta} = 0.9$
0.1	2.2982 (186)	2.2983 (114)	2.2983 (69)	2.2983 (57)	2.2983 (51)	2.2983 (39)	2.2983 (36)
0.2	2.2983 (114)	2.2983 (69)	2.2983 (39)	2.2983 (33)	2.2983 (27)	2.2983 (27)	2.2983 (27)
0.5	2.2983 (57)	2.2983 (33)	2.2983 (27)	2.2983 (48)	2.2983 (144)	2.2983 (42)	–
0.7	–	2.2983 (30)	2.2983 (81)	–	–	–	–
0.9	–	2.2983 (27)	–	–	–	–	–

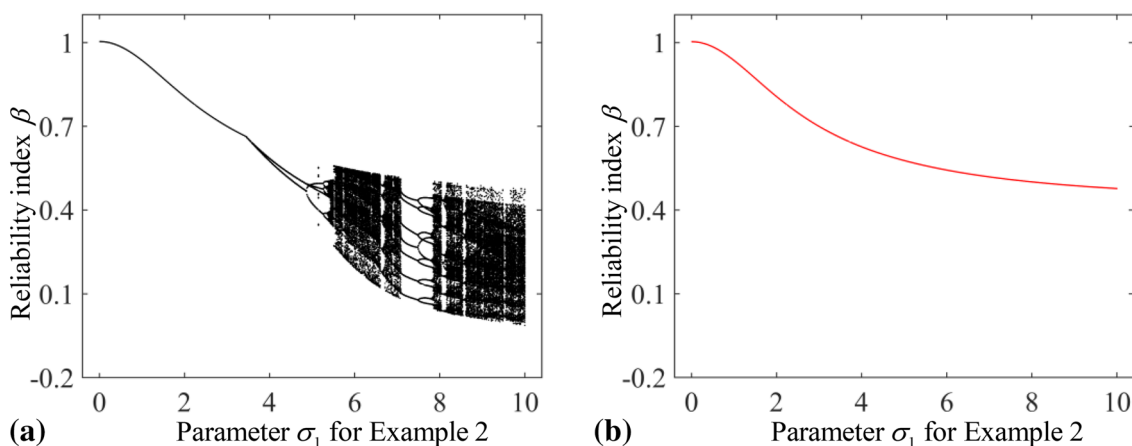


Fig. 8 a Bifurcation plot of reliability index of Example 2 using the HL–RF algorithm. b Chaos control of the HL–RF algorithm of Example 2 using STM and EASTM

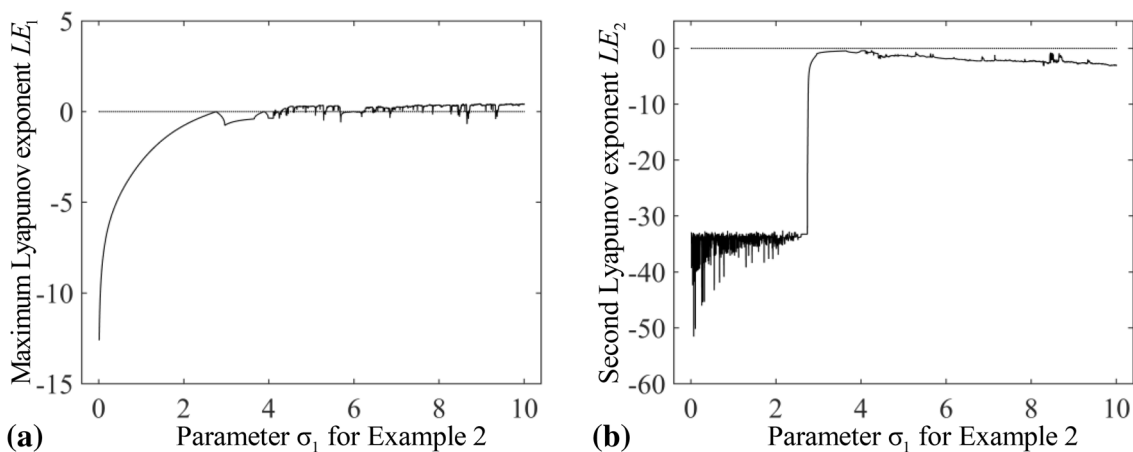


Fig. 9 Two Lyapunov exponents of the HL–RF algorithm for Example 2

Table 3 The number of function evaluations of different algorithms for Example 2

Methods	MPFP	Iterations	F evaluations	β	β^{MCS}
HL–RF	–	–	–	–	3.0707
iHL–RF	(1.7113, 2.3256)	21	247	2.8873	3.0707
STM	(1.7113, 2.3256)	202	606	2.8873	3.0707
DSTM	(1.7113, 2.3256)	50	150	2.8873	3.0707
LFR	(2.5518, 2.1336)	31	93	3.3262	3.0707
ASTM	(1.7113, 2.3256)	13	47	2.8873	3.0707
EASTM	(1.7113, 2.3256)	13	39	2.8873	3.0707

of HL–RF algorithm. The bifurcation plot of reliability index of HL–RF algorithm and two Lyapunov exponents is, respectively, given in Figs. 8 and 9, which is identical to reference [20]. It is seen that the reliability index β shows the bifurcation, chaos and periodic oscillation phenomena as the change of standard deviation σ_1 , and the Lyapunov exponents reflect these phenomena strictly. In addition, MCS is used to verify outcomes of different methods with a ten-million sample size, and the results are listed in Table 3, and the reliability index is 3.0707.

The results of different algorithms are listed in Table 3. It is shown that FORM method has some errors for highly nonlinear limit state function. All methods except HL–RF iterative algorithm converge to the same optimum. iHL–RF and STM are robust but inefficient. DSTM is more efficient than iHL–RF, STM and LFR using the directional chaos

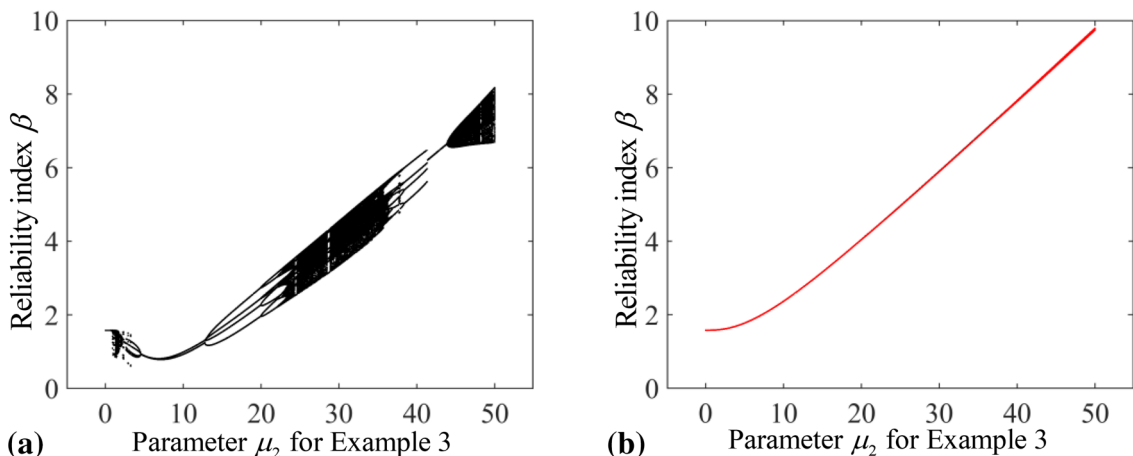


Fig. 10 a Bifurcation plot of reliability index of Example 3 using the HL–RF algorithm. b Chaos control of the HL–RF algorithm of Example 3 using STM and EASTM

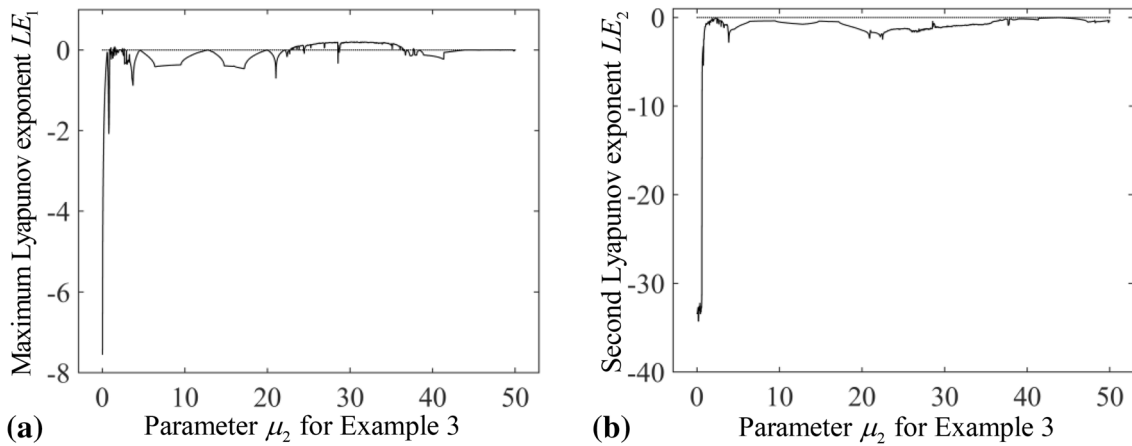


Fig. 11 Two Lyapunov exponents of the HL–RF algorithm for Example 3

Table 4 The number of function evaluations of different algorithms for Example 3

Methods	MPFP	Iterations	F evaluations	β	β^{MCS}
HL–RF	–	–	–	–	2.9038
iHL–RF	(1.8158, 1.4617)	53	745	2.3654	2.9038
STM	(1.8158, 1.4617)	241	723	2.3655	2.9038
DSTM	(1.8158, 1.4617)	21	63	2.3655	2.9038
LFR	(1.8158, 1.4617)	35	105	2.3655	2.9038
ASTM	(1.8158, 1.4617)	12	92	2.3655	2.9038
EASTM	(1.8158, 1.4617)	12	36	2.3655	2.9038

control strategy. Comparing with STM and DSTM, the efficiency of ASTM is improved significantly by finding a suitable chaos control factor, and the number of function calls for calculating chaos control factor is eight times. EASTM is the most efficient method by updating the chaos control factor adaptively.

Example 3 $g_3 = X_1^4 + X_2^4 + X_2^4 - 20$, in which X_1 and X_2 represent the random variables with normal distribution, $\mu_1 = 10, \mu_2 = 10, \sigma_1 = \sigma_2 = 5$ [20].

The mean μ_2 is deemed as the control parameter, which is used to demonstrate the convergence of HL–RF algorithm. The bifurcation plot of reliability index of HL–RF algorithm and two Lyapunov exponents is given in Figs. 10 and 11, respectively, which is identical to reference [20]. It is seen that the reliability index β shows the bifurcation, chaos and periodic oscillation phenomena as the change of mean μ_2 , and the Lyapunov exponents reflect these phenomena strictly. In addition, MCS is used to verify outcomes of different methods with a 10-million sample size, and the results are listed in Table 4. It is shown that FORM method has some errors for highly nonlinear limit state function.

The results of different algorithms are listed in Table 4. It is shown that FORM method has some errors for highly nonlinear limit state function. All methods except HL–RF iterative algorithm converge to the same optimum. iHL–RF and STM are robust but inefficient. LFR is more efficient than iHL–RF and STM. DSTM shows the high efficiency, but how to find a proper chaos control factor is questionable. Both ASTM and EASTM are very efficient. Since EASTM only obtains the approximate MPTP during each iterative step, it is more efficient than ASTM.

Table 5 The number of function evaluations for Example 4

Methods	MPFP	Iterations	F evaluations	β	β^{MCS}
HL–RF	–	–	–	–	1.3810
iHL–RF	(14.8387, 25.0441, 0.8667, 0.0466)	17	314	1.0256	1.3810
STM	(14.7909, 25.0440, 0.8622, 0.0468)	89	445	1.0256	1.3810
DSTM	(14.8622, 25.0925, 0.8620, 0.0479)	36	180	1.0255	1.3810
LFR	(14.8349, 25.0452, 0.8669, 0.0468)	9	45	1.0256	1.3810
ASTM	(14.8389, 25.0419, 0.8666, 0.0466)	7	51	1.0256	1.3810
EASTM	(14.8389, 25.0436, 0.8666, 0.0467)	9	45	1.0256	1.3810

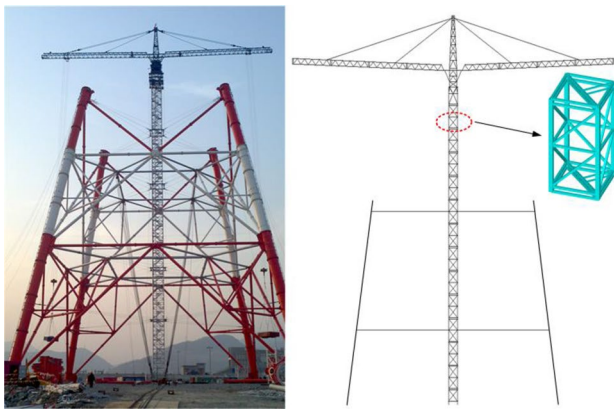


Fig. 12 A tower crane

Example 4 This reliability analysis example was studied by many researchers (Liu and Der Kiureghian [29]; Yang et al. [19]; Yang [24]). The performance function is obtained by response surface method.

$$g_4 = 1.1 - 0.00115X_1X_2 + 0.00157X_2^2 + 0.00117X_1^2 + 0.0135X_2X_3 - 0.0705X_2 - 0.00534X_1 - 0.0149X_2X_3 - 0.0611X_2X_4 + 0.0717X_1X_4 - 0.226X_3 + 0.0333X_3^2 - 0.558X_3X_4 + 0.998X_4 - 1.339X_4^2,$$

where random variables X_1, X_2 and X_3 follow normal distribution ($\mu_1 = 10, \sigma_1 = 5, \mu_2 = 25, \sigma_2 = 5, \mu_3 = 0.8, \sigma_3 = 0.2$). Random variable X_4 follows lognormal distribution ($\mu_4 = 0.0625, \sigma_4 = 0.0625$).

HL–RF algorithm obtains periodic solutions, and the Lyapunov exponents are $(-0.1266, -1.2681, -1.7133, -3.5744)$. So it reflects the chaotic phenomenon of HL–RF algorithm clearly. To address this issue, advanced algorithms (*i*HL–RF, STM, DSTM, LFR, ASTM and EASTM) are employed, and the results of all these algorithms are listed in Table 5. The MCS is used to validate the accuracy of different algorithms with a 10-million sample size. It is seen that all these algorithms except HL–RF can satisfy

Table 7 Different stopping criteria for all examples

Methods	Example 1	Example 2	Example 3	Example 4
$\epsilon = 10^{-3}$				
HL–RF	–	–	–	–
<i>i</i> HL–RF	2.2982 (203)	2.8873 (226)	2.3610 (539)	1.0256 (237)
STM	2.2980 (468)	2.8860 (468)	2.3652 (582)	1.0227 (240)
DSTM	2.2982 (57)	2.8871 (111)	2.3654 (57)	1.0167 (70)
LFR	2.2983 (48)	3.3283 (36)	2.3655 (93)	1.0256 (35)
ASTM	2.2982(38)	2.8873 (37)	2.3655 (92)	1.0256 (44)
EASTM	2.2983 (24)	2.8873 (33)	2.3655 (33)	1.0256 (35)
$\epsilon = 10^{-5}$				
HL–RF	–	–	–	–
<i>i</i> HL–RF	2.2983 (301)	2.8873 (324)	2.3655 (850)	1.0256 (314)
STM	2.2982 (741)	2.8873 (741)	2.3655 (858)	1.0256 (650)
DSTM	2.2983 (93)	2.8873 (189)	2.3655 (66)	1.0256 (400)
LFR	2.2983 (66)	3.3262 (54)	2.3655 (105)	1.0256 (70)
ASTM	2.2983 (43)	2.8873 (57)	2.3655 (97)	1.0256 (65)
EASTM	2.2983 (30)	2.8873 (45)	2.3655 (42)	1.0256 (55)
$\epsilon = 10^{-7}$				
HL–RF	–	–	–	–
<i>i</i> HL–RF	2.2983 (441)	2.8873 (349)	2.3655 (997)	1.0256 (1092)
STM	2.2983 (1011)	2.8873 (1011)	2.3655 (1123)	1.0256 (1105)
DSTM	2.2983 (132)	2.8873 (270)	2.3655 (75)	1.0256 (885)
LFR	–	–	–	1.0256 (125)
ASTM	2.2983 (43)	2.8873 (77)	2.3655 (102)	1.0256 (93)
EASTM	2.2983 (51)	2.8873 (60)	2.3655 (48)	1.0256 (100)
$\epsilon = 10^{-9}$				
HL–RF	–	–	–	–
<i>i</i> HL–RF	2.2983 (652)	2.8873 (374)	2.3655 (1317)	1.0256 (2113)
STM	2.2983 (1281)	2.8873 (1281)	2.3655 (1395)	1.0256 (1585)
DSTM	2.2983 (168)	2.8873 (351)	2.3655 (81)	1.0256 (1460)
LFR	–	–	–	1.0256 (185)
ASTM	2.2983 (48)	2.8873 (102)	2.3655 (102)	1.0256 (135)
EASTM	2.2983 (66)	2.8873 (75)	2.3655 (57)	1.0256 (150)

the accuracy requirement. *i*HL–RF and STM are robust but inefficient, in which *i*HL–RF algorithm requires many computational cost to find MPFP. DSTM is more efficient

Table 6 The number of function evaluations for tower crane

Methods	MPFP	Iterations	F evaluations	β	β^{MCS}
HL–RF	(1.9758 × 10 ⁵ , 2.8002, 188.32, 109.16)	16	80	2.2462	2.2464
<i>i</i> HL–RF	(1.9761 × 10 ⁵ , 2.8001, 195.42, 109.16)	3	22	1.9377	2.2464
STM	(1.9803 × 10 ⁵ , 2.8002, 187.66, 109.11)	78	312	2.2436	2.2464
DSTM	(1.9766 × 10 ⁵ , 2.8001, 188.94, 109.16)	4	20	2.2421	2.2464
LFR	(1.9765 × 10 ⁵ , 2.8002, 188.96, 109.73)	41	205	2.2572	2.2464
ASTM	(1.9766 × 10 ⁵ , 2.8002, 189.09, 109.16)	6	71	2.2462	2.2464
EASTM	(1.9765 × 10 ⁵ , 2.7991, 187.75, 109.16)	10	50	2.2462	2.2464

than *i*HL–RF and STM using the directional chaos control strategy. EASTM and LFR are efficient than other advanced algorithms. Although the number of iterations of ASTM is less than that of EASTM, it needs to call the performance function 16 times to determine the chaos control factor, and thus the computational cost of EASTM is more than that of EASTM.

Example 5 A tower crane.

A tower crane with $87\text{ m} \times 1.52\text{ m} \times 1.52\text{ m}$ is shown in Fig. 12, which is extensively used for lifting materials in construction sites. The entire tower cranes are composed by 29 standard components, and each component is composed by 32 bars. The sectional dimension of vertical bar is $120 \times 10\text{ mm}$, while the sectional dimension of cross bar is $70 \times 5\text{ mm}$. Four random variables, including Young's modulus, Poisson's ratio, windward wind load and transverse wind load are considered. The means and coefficient of variations for these four random parameters are [206 Gpa, 2.8, 172.29 kN, 109.16 kN] and [0.02, 0.02, 0.1, 0.1], respectively. The maximum lifting weight is 7.6 t , and the performance function is defined as follows:

$$g_5 = 0.75 - \Delta,$$

where Δ denotes the maximum displacement, which should be less than 0.75 m.

The results of different algorithms, including the values of MPFP, iterative numbers and the number of function calls, are given in Table 6. The MCS is performed with 1.5×10^4 samples, and the reliability index is 2.2464. According to the results shown in Table 6, *i*HL–RF, STM, DSTM and LFR show inaccuracy, while other methods are converged accurately with reliability index 2.2462. ASTM is more

efficient than HL–RF and is more accurate than *i*HL–RF, STM, DSTM and LFR, and it calls the performance function 41 times to search the chaos control factor. Comparing with ASTM, the efficiency of EASTM is further enhanced in this example.

Since the convergence is also impacted by stopping criterion, four different stopping criterion values, i.e., 10^{-3} , 10^{-5} , 10^{-7} and 10^{-9} , are used for all benchmark examples, and the computational results are listed in Table 7. HL–RF algorithm cannot find the correct reliability index. STM is very robust but inefficient. DSTM and LFR are very efficient; however, LFR appears oscillatory and cannot converge when the stopping criterion is too small. ASTM and EASTM are more efficient and robust than other existing methods. To show this, the iterative histories of Examples 3 and 4 with stopping criterion $\varepsilon = 10^{-7}$ are given in Fig. 13 as a representative. It is observed that HL–RF method generates periodic-2 solutions. For Example 3, the iterative points of LFR meet the convergence problem and oscillate slightly around the MPFP. ASTM and EASTM are more efficient than other methods. Since ASTM needs solving the optimization model to determine the chaos control factor, the number of iterations of ASTM is less than that of EASTM.

8 Conclusions

In this study, two effective iterative algorithms are developed to enhance the efficiency and robustness of most probable failure point (MPFP) search algorithm via transforming it to solving a series of MPTPs. Adaptive stability transformation method (ASTM) is proposed to improve the performance of HL–RF algorithm. Then, the proposed method is enhanced using the most probable target point (MPTP) approximation, which is named as enhanced

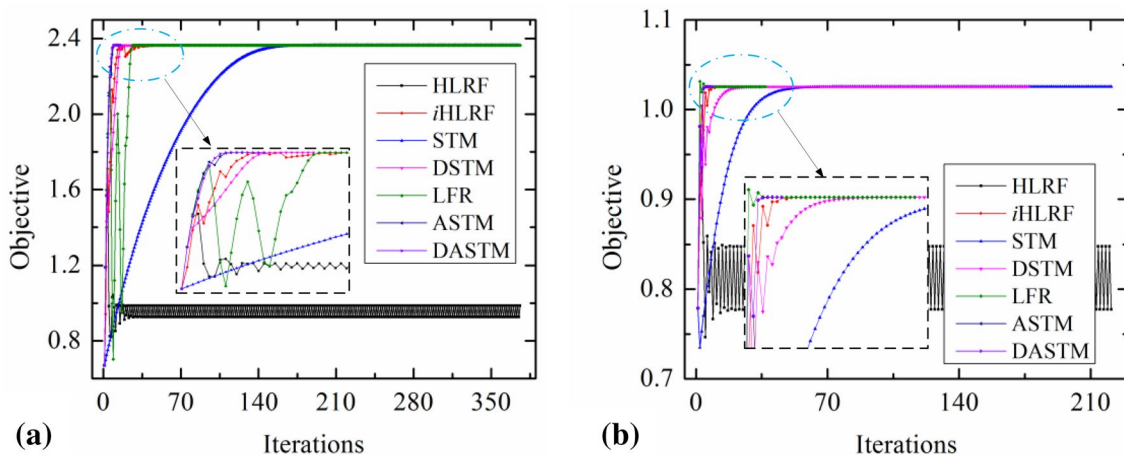


Fig. 13 Iterative history with stopping criterion $\varepsilon = 10^{-7}$. **a** Example 3, **b** Example 4

adaptive stability transformation method (EASTM). The proposed ASTM and EASTM show high performance in terms of efficiency and robustness.

Moreover, the performances of two proposed algorithms are tested by five benchmark examples. The results of ASTM and EASTM are compared to five popular reliability algorithms, including HL–RF iterative algorithm, *i*HL–RF iterative algorithm, stability transformation algorithm (STM) and directional stability transformation algorithm (DSTM) and limited Fletcher–Reeves (LFR) algorithm. Results reveal that ASTM and EASTM can find the accurate MPFP with less computational cost. The application of ASTM and EASTM for other nonlinear engineering problems will be promising in future.

Acknowledgements The supports of the National Natural Science Foundation of China (Grant Nos. 11602076 and 51605127), the Natural Science Foundation of Anhui Province (No. 1708085QA06) and the Fundamental Research Funds for the Central Universities of China (No. JZ2016HGBZ0751) are much appreciated.

References

- Rashki M, Miri M, Azhdary MM (2012) A new efficient simulation method to approximate the probability of failure and most probable point. *Struct Saf* 39(11):22–29
- Lee IJ, Shin J, Choi KK (2013) Equivalent target probability of failure to convert high-reliability model to low-reliability model for efficiency of sampling-based RBDO. *Struct Multidiscip Optim* 48(2):235–248
- Keshtegar B, Baharom S, El-Shafie A (2017) Self-adaptive conjugate method for a robust and efficient performance measure approach for reliability-based design optimization. *Eng Comput*. <https://doi.org/10.1007/s00366-017-0529-7>
- Zhang D, Han X, Jiang C, Liu J, Li Q (2017) Time-dependent reliability analysis through response surface method. *J Mech Des* 139(4):041404
- Lim J, Lee B, Lee I (2016) Post optimization for accurate and efficient reliability-based design optimization using second-order reliability method based on importance sampling and its stochastic sensitivity analysis. *Int J Numer Meth Eng* 107(2):93–108
- Jiang C, Han S, Ji M, Han X (2015) A new method to solve the structural reliability index based on homotopy analysis. *Acta Mech* 226(4):1067–1083
- Du XP, Chen W (2004) Sequential optimization and reliability assessment method for efficient probabilistic design. *J Mech Des* 126(2):225–233
- Li G, Meng Z, Hu H (2015) An adaptive hybrid approach for reliability-based design optimization. *Struct Multidiscip Optim* 51(5):1051–1065
- Rashki M, Miri M, Moghaddam MA (2014) A simulation-based method for reliability based design optimization problems with highly nonlinear constraints. *Autom Constr* 47(11):24–36
- Meng Z, Zhou HL, Li G, Hu H (2017) A hybrid sequential approximate programming method for second-order reliability-based design optimization approach. *Acta Mech* 228(5):1965–1978
- Lee JO, Yang YS, Ruy WS (2002) A comparative study on reliability-index and target-performance-based probabilistic structural design optimization. *Comput Struct* 80(3–4):257–269
- Meng Z, Li G, Wang BP, Hao P (2015) A hybrid chaos control approach of the performance measure functions for reliability-based design optimization. *Comput Struct* 146(1):32–43
- Hasofer AM, Lind NC (1974) Exact and invariant second moment code format. *J Eng Mech Div Asce* 100(1):111–121
- Rackwitz R, Fiessler B (1978) Structural reliability under combined random load sequences. *Comput Struct* 9(5):489–494
- Zhang Y, Der Kiureghian A (1995) Two improved algorithms for reliability analysis. *Reliability and optimization of structural systems*. Springer, Berlin, pp 297–304
- Periçaro GA, Santos SR, Ribeiro AA, Matioli LC (2015) HLRFBFGS optimization algorithm for structural reliability. *Appl Math Model* 39(7):2025–2035
- Lopez RH, Torii AJ, Miguel LFF, Souza Cursi JE (2015) Overcoming the drawbacks of the FORM using a full characterization method. *Struct Saf* 54(5):57–63
- Santos SR, Matioli LC, Beck AT (2012) New optimization algorithms for structural reliability analysis. *Cmes Comp Model Eng* 83(1):23–55
- Yang DX, Li G, Cheng GD (2006) Convergence analysis of first order reliability method using chaos theory. *Comput Struct* 84(8–9):563–571
- Meng Z, Li G, Yang DX, Zhan L (2017) A new directional stability transformation method of chaos control for first order reliability analysis. *Struct Multidiscip Optim* 55(2):601–612
- Keshtegar B (2017) A hybrid conjugate finite-step length method for robust and efficient reliability analysis. *Appl Math Model* 45(5):226–237
- Keshtegar B (2016) Chaotic conjugate stability transformation method for structural reliability analysis. *Comput Methods Appl Mech Eng* 310:866–885
- Keshtegar B (2017) Limited conjugate gradient method for structural reliability analysis. *Eng Comput* 33(3):621–629
- Yang DX (2010) Chaos control for numerical instability of first order reliability method. *Commun Nonlinear Sci Numer Simul* 15(10):3131–3141
- Tu J, Choi KK, Park YH (1999) A new study on reliability-based design optimization. *J Mech Des* 121(4):557–564
- Petkov BH, Vitale V, Mazzola M, Lanconelli C, Lupi A (2015) Chaotic behaviour of the short-term variations in ozone column observed in Arctic. *Commun Nonlinear Sci Numer Simul* 26(1–3):238–249
- Pingel D, Schmelcher P, Diakonou FK (2004) Stability transformation: a tool to solve nonlinear problems. *Phys Rep* 400(2):67–148
- Schmelcher P, Diakonou FK (1998) General approach to the localization of unstable periodic orbits in chaotic dynamical systems. *Phys Rev E* 57(3):2739–2746
- Liu PL, Der Kiureghian A (1991) Optimization algorithms for structural reliability. *Struct Saf* 9(3):161–177